NÖHÜ Müh. Bilim. Derg. / NOHU J. Eng. Sci., 2023; 12(2), 626-636

Niğde Ömer Halisdemir Üniversitesi Mühendislik Bilimleri Dergisi
Niğde Ömer Halisdemir University Journal of Engineering Sciences

Araştırma makalesi / Research article

www.dergipark.org.tr/tr/pub/ngumuh / www.dergipark.org.tr/en/pub/ngumuh

Spatio-temporal change detection of built-up areas with Sentinel-1 SAR data using random forest classification for Arnavutköy Istanbul

Sentinel-1 verilerine rastgele orman sınıflandırma yaparak İstanbul Arnavutköy için yapılaşma alanlarının konumsal ve zamansal değişiminin tespiti

Hasan Bilgehan Makineci[1,*]

[1] *Konya Technical University, Geomatics Engineering Department, 42130, Konya, Türkiye*

Abstract

As one of the most populated cities in Turkiye and the world, the Istanbul metropolis has always attracted the crowd of people masses. Arnavutköy Town has become one of the critical points of Istanbul City with increasing built-up areas (BAs). The spatial-temporal change detection of the expansion of the BAs of this district is essential data on behalf of Istanbul City. This research aims to determine urban areas expansion zones, also defined as the BAs footprint, from Sentinel-1 radar data. The determination of Sentinel-1A data of the urban area change detection encountered in Arnavutköy Town between 2018-2021 with Random Forest (RF) classification machine learning algorithm is investigated in this study. Based on the changes in spatial-temporal data, the direction of urban development has been determined. In addition, to visually compare the Normalized Difference Built-up Index (NDBI) and optical Sentinel-2A's false color urban RGB composite, which is a distinct data format, the processes have been proved. As a result of the study, SAR satellite data was found to be more appropriate than optical satellite data since not being affected by atmospheric conditions for extracting BAs with remotely sensed data.

Keywords: Built-up areas extraction; Change detection, NDBI, Sentinel-1A, Random forest classification

Öz

Türkiye'nin ve dünyanın en kalabalık şehirlerinden biri olan İstanbul, her zaman kitleler halinde insanları kendine çekmiştir. Arnavutköy, artan Yapılaşma Alanları (YA'lar) ile İstanbul şehrinin kritik ilçelerinden biri haline gelmiştir. Bu ilçenin YA'larının genişlemesinin konumsal ve zamansal değişiminin tespiti, İstanbul adına önemli bir ihtiyaçtır. Bu çalışma, Sentinel-1 radar verilerinden YA ayak izi olarak da tanımlanan kentsel alanların genişleme bölgelerini belirlemeyi amaçlamaktadır. Bu çalışmada, 2018-2021 yılları arasında Arnavutköy Kasabasında karşılaşılan kentsel alan değişim tespitinin Sentinel-1A verilerinden makine öğrenmesi algoritması olan Rastgele Orman (RO) sınıflandırıcısı ile belirlenmesi incelenmiştir. Konumsal-zamansal verilerde yaşanan değişimlerden yola çıkarak, kentsel gelişimin yönü belirlenmiştir. Ayrıca, Normalize Fark Yapı İndeksi (NDBI) ve Sentinel-2A yalancı renkli RGB kompoziti görsel olarak kullanılarak karşılaştırmalı olarak yapısal değişim kanıtlanmıştır. Çalışma sonucunda uzaktan algılanan verilerle YA'ların çıkarılması konusunda, SAR uydu verilerinin atmosferik koşullardan etkilenmediği için optik uydu verilerine göre daha uygun olduğu belirlenmiştir.

Anahtar kelimeler: Yapılaşma alanları çıkarımı; Değişim analizi, NDBI, Sentinel-1A, Rastgele orman sınıflandırması

1 Introduction

The world population has been migrating heavily to big cities for the last fifty years [1, 2]. Significant metropolises such as Tokyo, London, Los Angeles, and Istanbul are exposed to international migration from the surrounding provinces and regular/irregular migrants. Urbanization is increasing fast since living conditions are better than in rural areas, and there are more job opportunities. As a result, unplanned settlements occur in megacities, so forest areas, consumable water resources, and natural habitats of different species are under threat [3, 4]. Local municipalities and governments' decision-making mechanisms should focus on megacities' sustainable and logical urban development, and these should be one of the most critical issues [5].

It is known that collecting detailed information in an appropriate way on Built-up Areas (BAs) is fundamental for getting precautions against natural hazards (e.g., earthquakes, tsunamis, etc.) response strategies [6, 7]. Earth observation with remote sensing technique is an essential instrument for obtaining data on the features and improvement of BAs. Compared with optical sensors, synthetic aperture radar (SAR) systems can preferably because that system works both day and night and under all weather conditions [8, 9]. This yields more substantial data in cloudy and rainy regions as opposed to optical images. The SAR applications concerning settlement change detection, population growth estimation, analyzing urban mapping and land-use patterns, and monitoring socioeconomic characteristics have been represented in many studies before [10, 11]. Although SAR data do not strongly extract information on all kinds of structures because of the complexity of evaluating BAs [12],

* Sorumlu yazar / Corresponding author, e-posta / e-mail: hbmakineci@ktun.edu.tr (H. B. Makineci)
Geliş / Recieved: 12.11.2022 Kabul / Accepted: 17.03.2023 Yayımlanma / Published: 15.04.2023
doi: 10.28948/ngmuh.1203301

improvements have been made in extracting civilized town areas with high-resolution SAR data [13]. Advantages have reviewed SAR-based BAs-extraction methods on outcomes with MachineLearning (ML) methods [10, 14, 15] such as support vector machine (SVM) [16], Artificial Neural Network (ANN) [17, 18], and Random Forest (RF) [19-22]. Some researchers have created an Urban Extractor to estimate SAR data for global urban mapping using a processing chain [23]. The defined workflow involves post-processing, which has many enhancements to an existing technique, and urban extraction based on spatial indices and Gray Level Co-occurrence Matrix (GLCM) textures [24]. As show the reliability of the modified technique, ENVISAT Advanced Synthetic Aperture Radar (ASAR) C-VV data at 30 m resolution were selected over ten metropolitan areas and a rural area from six continents [25]. The results determine that the KTH-Pavia Urban Extractor expertly selects urban areas and small towns from ENVISAT ASAR data. Additionally, BAs may be accurately mapped at 30 m resolution with just one or two SAR data. However, the method takes a while to run when GLCM texture features are used. [26]. A study proposes a BAs extraction method that combines nighttime light images and point of interest (POI) data. With that approach, they use nighttime light data and POI data to extract BAs and use a mathematical morphology-based method to merge them [27]. Since POI data have relatively accurate location information and a high spatial correlation with BAs, the proposed fusion method overcomes low resolution and overflow problems found in extraction methods based solely on nighttime light data [28, 29].

Sentinel-1 allows for time-series observations by turning two satellites on 12-day repeated cycles for global data [30]. Sentinel-1 data have been used for BAs extraction, land cover classification [31-33], and forest monitoring [34]. Sentinel-1A data usually performs well on localized growth map production with C-B and wavelength. In addition to this, Sentinel-1A offers a unique possibility to develop a service for detecting BAs at a global scale with its freely available data [35]. Sentinel-1 time series data have been used in several kinds of research with hopeful outcomes for change detection [36, 37].

BAs extraction from optical multispectral (MSI) satellite data is a preferred method. Especially with the use of different indexes, change detection of urban areas from high-resolution remote sensing satellite data is one of the popular topics of recent years. Enhanced Built-Up and Bareness Index (EBBI) and Normalized Difference Built-up Index (NDBI) are the most commonly used indexes in the literature [38-40].

This study aimed to evaluate the applicability of a BAs extraction and change detection approach using multiple time-series observations of Sentinel-1A Single Look Complex (SLC) data based on an ML algorithm in the Arnavutköy Town of İstanbul City, Turkey. Change detection and Regional Growing (RG) models were created for each observation (from years between 2018 and 2021) of Sentinel-1 using a Random Forest algorithm (RF). Subsequently, BAs extraction at each pixel position was detected using the estimated time series of change probabilities [41]. The process may not be entirely suitable for BAs extraction with a modest resolution, approximately 20-30 m SAR data. Moreover, surfaces in BAs are much more distinct in data with higher resolution than in data with 30 m resolution, so extracting BAs only on coherence can lower overall accuracy. In this research, to overcome that difficulty, additional spatial and vectorial construction features are introduced using Sentinel-1 SLC data from coherence with RF algorithm. This research aims to generate a sustainable and momentarily method from Sentinel-1 SLC SAR data on the extraction step for proper BAs outcomes. In addition, false color urban RGB composite obtained from optical Sentinel-2A, which is a different data type, and the NDBI were visually compared in order to verify the operations performed. Thus, rough errors were avoided, and it was determined that SAR satellite data was more suitable than optical satellite data (due to not being affected by atmospheric conditions). Also, to see and evaluate how the region will take shape in the future, the 1/100.000 scaled environmental plan of the European side of Istanbul has been digitised and used in practice and analysis. The success of the suggested approach was tested in the fast-growing settlement area Arnavutköy Town, İstanbul, over Turkiye, including a wide variety of natural environments (water bodies, natural forests, etc.) and structural building types (airport, factories, high-rise buildings, detached houses, etc.). The contribution of this research to the literature is to monitor uncontrolled BAs in critically important districts of metropolitan cities through temporal analyses with multiple SAR data. Another contribution is to assure that a robust algorithm such as RF gives high-accuracy results in classification and analyses reliable results.

2 Material and methods

In this section, the methods and materials applied in the rest of the research are mentioned.

2.1 Study area

The rapid growth of world-renowned metropolises is, such as Istanbul, contingent on the supply-demand balance. The sustainability of population growth is a challenging situation in limited land conditions. For this reason, agricultural areas, forest areas, etc., regions that do not concur with construction are forced to settle plans to respond to demands [4, 42].

Istanbul City has a transitional climate with temperate, subtropical, Mediterranean, and oceanic climates, according to the Köppen climatic classification. Separate microclimates can be found in the city because of its size, topography, and coastline that faces two different seas in the north and south. A temperate subtropical and oceanic climate with relatively high humidity occurs in the areas that make up the city's northern half, near the Black Sea and the coasts of the Bosphorus [43]. Istanbul experiences hot, humid summers and cool, rainy, and occasionally snowy winters. The air may feel colder than it actually is because of the humidity, which makes it warmer than it actually is. Rain and snow are typical winter weather, and temperatures range from 2 to 9 °C. The typical summertime highs are 18 to 28

℃, and flooding and rain are expected. The two hottest months, with an average temperature of 23 °C, are July and August. With an average temperature of 5 °C, January and February are the coldest months [44, 45].

Considering its climatic features and land use situation, Istanbul City is a city that is growing rapidly in terms of structure and where the construction is continuous except in the winter season. In the winter seasons, generally, when the construction is static, remote sensing data analysis is not perfectly appropriate due to meteorological events such as clouds, snowy lands, fog, and rain. The situation is almost the same, especially in Arnavutköy, as in Istanbul in general. Located in the west of Istanbul (known as the European Side), the district has the Black Sea Coast (Figure 1). The latest construction of the Great Istanbul Airport and the Canal Istanbul Project planned to be built in the future are in Arnavutköy Town.

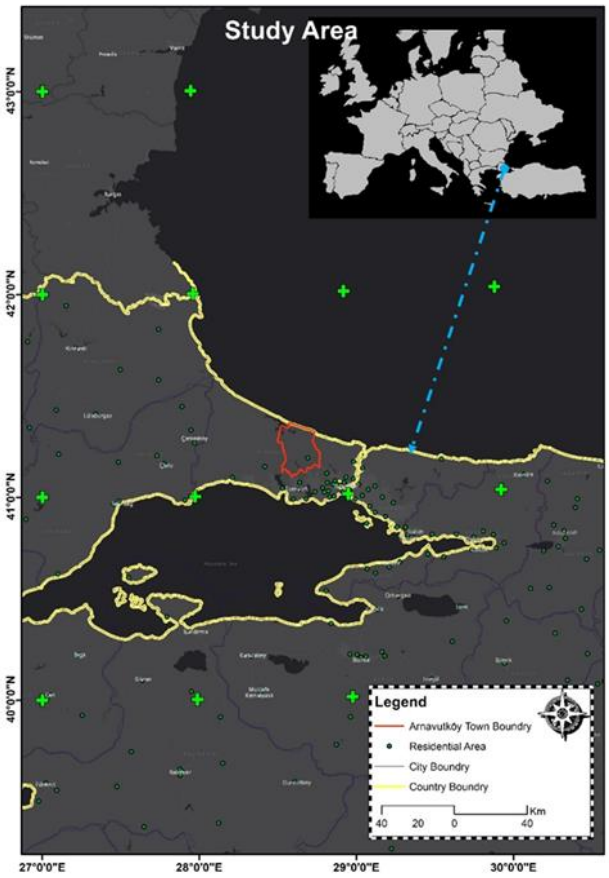

Figure 1. The study area of research (red lined area: Arnavutköy Town)

2.2 SAR data used in study

The sentinel-1 mission is made up of two polar-orbiting satellites that each carry a single C-band synthetic-aperture radar (SAR) sensor that can operate in four different acquisition modes with varied resolutions (down to 5 m) and coverage (up to 400 km). In this study, the Interferometric Wide Swath (IWS) mode products at Level-1 Single Look Complex (SLC) were preferred [33]. The IW swath mode acquires a 250 km swath for SLC products with a spatial resolution of 5 to 20 meters. The wide-swath coverage is achieved using Terrain Observation by Progressive Scans (TOPS) [30]. This research presents a multi-temporal analysis, collecting data from February 2018 to April 2021 (Table 1). However, to achieve meaningful results with the same temporal baseline repeated coverage, only data derived from the Sentinel-1A within a twelve-day revisit time was considered. Since rapid urbanization in Arnavutköy Town, Istanbul, though the spatial resolution of the Sentinel-1 SAR data is not perfect for extracting urban footprint, the change of BAs detected in recent years cannot be disregarded. As a result, BAs can be considered fixed for all Sentinel-1 data obtained within a year. The Sentinel Open Access Hub has provided all of the Sentinel-1 data used in this research free of charge.

Table 1. The Sentinel-1 data specification

Acquisition Year	Acquisition Date	Temporal Baseline	Data Type
2018	26 February		Sentinel-1A IW SLC
	10 March	12 Days	
	22 March		
	03 April	12 Days	
	15 April		
	27 April	12 Days	
	09 May		
	21 May	12 Days	
2019	21 February		Sentinel-1A IW SLC
	05 March	12 Days	
	17 March		
	29 March	12 Days	
	10 April		
	22 April	12 Days	
	04 May		
	16 May	12 Days	
2020	11 March		Sentinel-1A IW SLC
	23 March	12 Days	
	04 April		
	16 April	12 Days	
	28 April		
	10 April	12 Days	
	22 May		
	03 June	12 Days	
2021	17 January		Sentinel-1A IW SLC
	29 January	12 Days	
	10 February		
	22 February	12 Days	
	06 March		
	18 March	12 Days	
	30 March	12 Days	

11 April

Since Istanbul City is in the northern hemisphere, construction activities generally become stable during winter. Therefore, winter and spring months were preferred for the analysis of BAs change with SAR data in order to give more accurate results for the annual structural follow-up and change detection analysis. However, it cannot be said that winter, the beginning of spring, and the end of autumn are the perfect period for obtaining optical satellite imagery from a meteorological point of view. This primary feature that distinguishes SAR data from optical satellite data proves why the study was carried out with SAR data.

2.3 Methodology

Complex preprocessing procedures that use SNAP software from the ESA are necessary for the use and temporal analysis of SAR data. However, such techniques begin with the standard preprocessing carried out on Sentinel-1 output in order to obtain interferometric coherence [46, 47].

2.3.1 Preprocessing of Sentinel-1A data

Sentinel-1 SAR data has two polarizations (VH and VV). The output coherence data comprises two different raster files related to the other polarizations. At the workflow process (Figure 2), it was identified one of the three sub-swaths from the original data subsequently selected only those bursts that cover the study area. Then, it was determined the coherence estimation. Finally, the "Range-Doppler Terrain Correction" was used, which involves using a digital elevation model (DEM) automatically downloaded from the SRTM auto-download library, choosing WGS84-UTM 36N as the projected coordinate system and specifying 15 m as an average output resolution [10, 19, 31, 46, 48, 49].

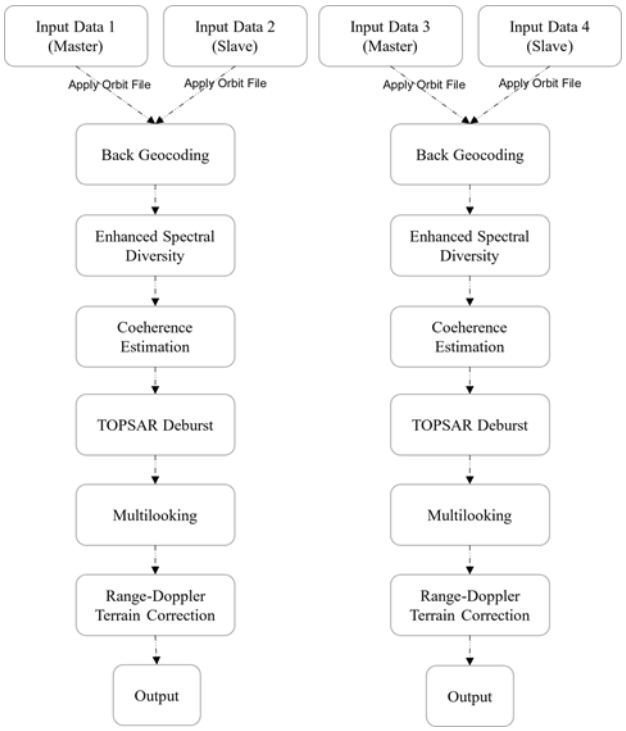

Figure 2. Workflow process of Sentinel-1A data on SNAP software

Using such a large number of SAR data increases the correlation between the data and the findings, helping to obtain more accurate results. On the other hand, the increased correlated findings obtained from SAR data provide high accuracy in classification with RF [50].

2.3.2 Built-up areas extraction and random forest algorithm

The RF algorithm has developed by combining the Bagging method [51] and the Random Subspace method. The basis of the algorithm is the evaluation of the predictions produced by multiple decision trees [52]. Each tree predicts a class, and the model prediction is the one that gets the most votes from the predicted classes. The RF algorithm consisting of 'n' trees is as in Figure 3.

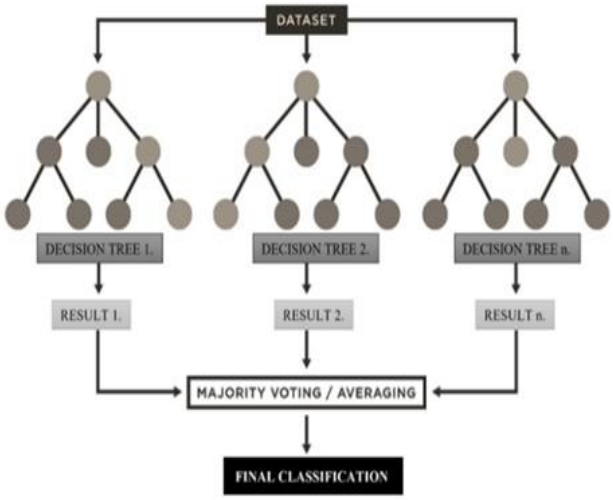

Figure 3. RF algorithm processing basics [51, 52]

In the supervised classification technique, the accuracy and the number of trees, nodes, branches, and leaves are directly proportional. In other words, the method's accuracy increases as the number of trees or other factors used in the method increases. On the contrary, the accuracy may decrease as the number of trees, and other factors decrease. Although RF and Decision Tree (DT) are similar in the algorithm, the main difference is that the formation of nodes and branches in RF occurs randomly. Therefore, as with other ML algorithms, some parameters must be determined beforehand to implement RF algorithm. These parameters are the number of trees to be created and the number of samples used in the node for each number of trees [3].

Sentinel-1A data became available for digitization after resampling at 15 m resolution. With this data, it is beneficial for extracting BAs to by applying supervised classification. The digitization process is defined as urban and non-urban in training and testing according to RF algorithm. Data set partitioning was preferred as 70% training set and 30% test set. According to the literature, the main reason for this preference is that the RF algorithm is shown as the training/test ratio with the highest success [18, 23, 51]. The

training dataset, together with the coherence estimated data, are presented in Figure 4.

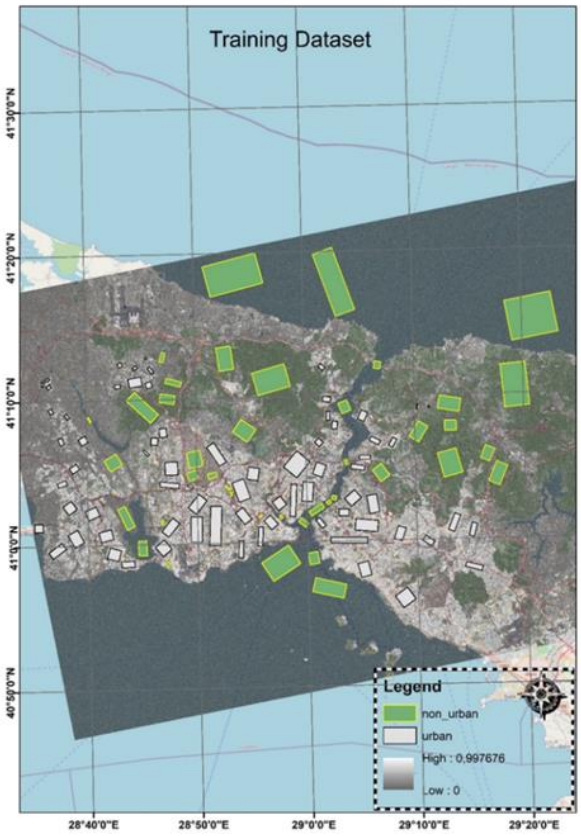

Figure 4. Training dataset of RF algorithm and coherence estimated processed data

2.3.3 *Post-processing*

After the training dataset of Sentinel-1 for all of Istanbul, the RF algorithm was started ideally. For RF testing, the algorithm was chosen the total samples as 1000 and the distribution of that samples as 50% Non-urban and 50% Urban area [19, 36, 52, 53, 54]. RF result conditions (Accuracy, Precision, Correlation, Error Rate, RMSE, Bias) for the 2018, 2019, 2020, and 2021 years are presented in Table 2. Indeed, the algorithm calculates those values by itself.

In order to list the general operations, first, Coherence Estimation data was obtained by using Sentinel-1A data for each year (divided into four masters and four slaves for each year). Next, urban and non-urban classes were created in the GIS software in order to classify the relevant data with RF. Then, training and testing processes were carried out with RF, and the results were revealed. Afterward, the generated rasters were visualized in GIS software and combined with the 1/100.000 scaled environmental plan of the reserve building area of the European side of Istanbul. Finally, after the essential operations such as clip, reprojection, and map algebra, the outcome maps obtained were evaluated, and the results were collected.

2.3.4 *Confirmation with Sentinel-2A data*

On account of determining the accuracy of the findings obtained from the research, high-resolution (10 m spatial resolution) multispectral (MSI) optical satellite images were acquired with Sentinel-2A. Sentinel-2 MSI sensor satellite missions with 13 spectral bands on 443-2190nm range, 290km frame width and 10m spatial resolution (four visible and near-infrared bands NIR), 20m (red edge and shortwave infrared band SWIR), and 60m (three atmospheric correction bands) offer free access optical remote sensing data used for also used for BAs extraction. To overcome obstacles in measurement, inspection, and process-monitoring applications—often unattainable with conventional technologies—imaging systems employing SWIR and NIR wavelength bands offer unique distant sensing capabilities [38-40]. The high-resolution difference between SAR data and Sentinel-2A data has led to using optical multispectral images as ground-truth data and the investigation of the accuracy of analyzes made with SAR data. It was also an excellent opportunity to show that SAR data are typically less affected by atmospheric conditions since the periods when BAs footprints are investigated are from winter to spring. The acquisition dates of the most suitable optical satellite images obtained on the dates determined in this study are shown in Table 3.

Table 3. The Sentinel-2 data specification

Acquisition Year	Acquisition Dates	Data Type
2018	07 June 2018	MSI L2A
2019	03 May 2019	MSI L2A
2020	17 April 2020	MSI L2A
2021	12 May 2021	MSI L2A

BAs extraction was performed with False Color Urban RGB (B12-B11-B4 combination) Composite and Normalized Difference Built-up Index (NDBI) from optical Sentinel-2 data. The NDBI is expressed as in Equation 1 [38].

$$NDBI = ((SWIR - NIR))/((SWIR + NIR)) \quad (1)$$

Table 2. Cross-validation assessments of RF for each year

Cross-validation (Number of Classes=2)		Accuracy (%)	Precision (%)	Correlation (%)	Error Rate (%)	RMSE (%)	Bias (%)	Year
Class 1	Non-urban	0.984	0.9734	0.9685	0.016	0.1265	-0.0112	2018
Class 2	Urban	0.984	0.9951	0.9685	0.016			
Class 1	Non-urban	0.9968	0.9956	0.9936	0.0032	0.0566	-0.0012	2019
Class 2	Urban	0.9968	0.998	0.9936	0.0032			
Class 1	Non-urban	0.9882	0.9841	0.9767	0.0118	0.1086	-0.0042	2020
Class 2	Urban	0.9882	0.9923	0.9767	0.0118			
Class 1	Non-urban	0.9976	0.996	0.9952	0.0024	0.049	-0.0016	2021
Class 2	Urban	0.9976	0.9992	0.9952	0.0024			

3 Results and discussion

As a result of ML, RMSE, and Bias values in Table 2 are within satisfactory limits as performing the RF algorithm [23, 51, 52, 53, 54]. The RF raster maps are imported into GIS software and made available for analysis. In this research, Arnavutköy Town boundaries were clipped in GIS software. The features and RF raster data in the boundaries of Arnavutköy Town obtained by digitizing the 1/100.000 scaled environmental plan of the reserve building area of the European side of Istanbul are combined and presented in a single display. The general workflow diagram representing these processes in order is presented in Figure 5. The resulting map produced and combined for each year subject to the research is seen in Figure 6.

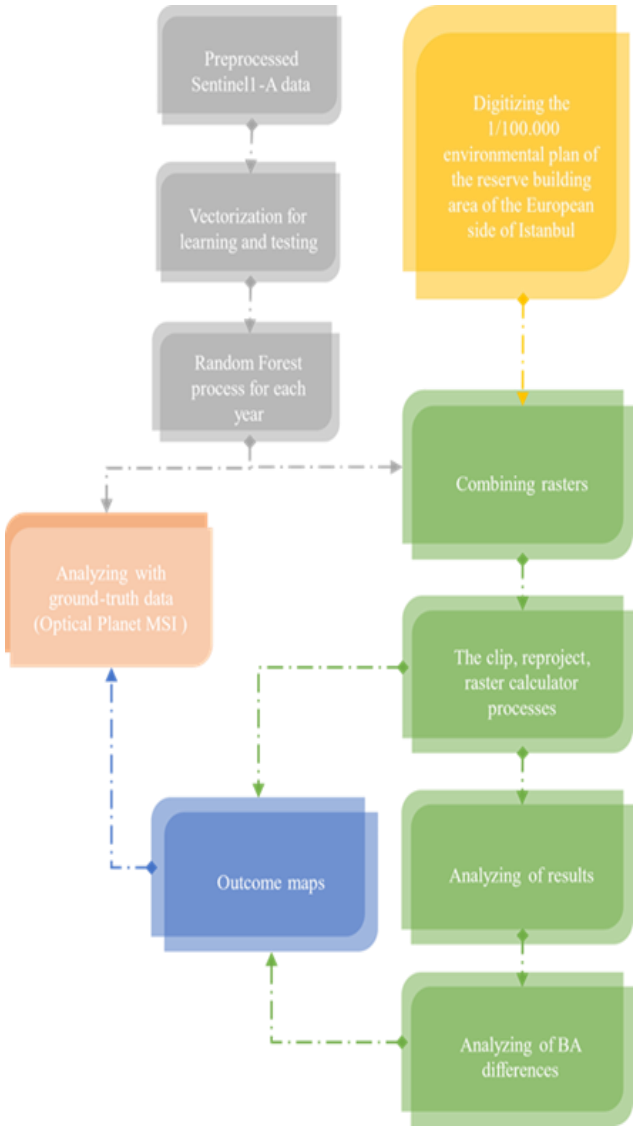

Figure 5. The workflow of research

To analyze the 15 m resampled RF raster maps, determining the differences between pixels was approved. This technique revealed the BAs differences in 2019, 2020, and 2021 by using 2018 as a basemap. As shown in Figure 7, where the differences are indicated, the constructed areas can be seen very clearly even with 15 m resolution data. The area converted as Arnavutköy Town boundaries in GIS software was calculated as 452 km^2. This area is expressed with a total of 2,013,721 pixels. While the RF raster map of 2018 is analyzed, it is related that the 696, and 122 pixel area is the BAs. Therefore, an additional BAs of 403,375 pixels was added in 2019. In addition, it has been determined that there are additional BAs in 2020 and 2021 with 536,490 and 553,284 pixels, respectively. The district's population was 270,549 in 2018, determined as 282,488 in 2019 and 296,709 in 2020. Since the population data is updated on 31 December of each year, the population information for 2021 is certainly not known. However, based on the annual population growth rate, approximately 310,000 are expected to live in the district in 2021 (Figure 7).

In 2018, BAs fields corresponded to 34.5% of the total area. However, with the increase in construction in 2019, the BAs was determined as 54.5% of the total area. Afterward, the increase continued in 2020 and 2021, and BAs were calculated as 61% and 62%, respectively.

Regions with more frequent BAs changes between 2018 and 2019 correspond to the north, northwest, and northeast regions of Arnavutköy Town center (Figure 8). This area, which can be defined as the neighborhood of Istanbul airport, has been opened for construction, especially for highways and the needs of the airport surroundings. Afterward, when examined between 2019 and 2020, the regions with more frequent BAs changes are the south of Arnavutköy Town center and its surroundings. Therefore, it is possible to say that the structuring for living people has increased, and the housing stock has caused the rise in BAs. Lastly, covering 2021 to 2020, the most frequently detected BAs changes are around the southwest, north, northeast, and east of Arnavutköy Town center.

In order to check the results, a visual evaluation was made with false color urban RGB composite, and the NDBI was obtained from Sentinel-2 optical data as a different data type (Figure 9). The Sentinel-2 data for 2018 is partially inaccurate due to cloud error, a common problem with optical satellite data. As seen in the URBAN RGB 2018 map in Figure 9, a part of the land can be detected due to cloud cover. Due to the higher spatial resolution of optical images, the areas with BAs are expected to be revealed more clearly. However, it can be seen when comparing Figure 8 and Figure 9 that SAR data is more successful in the BAs extraction process, thanks to the ability to receive day and night and not be affected by effects such as fog, cloud, and dust [38, 39].

As can be seen in Figure 7, Istanbul Airport initiates construction. Therefore, it would be relevant to state that the Kanal Istanbul project and the revised 1/100.000 scaled environmental plan of the reserve building area of the European side of Istanbul will increase with the construction of crowded human communities (from different nationalities) will come up to Arnavutköy Town. Just like in other towns of Istanbul, unplanned urbanization and irregular migration have been recognized as an urgent problem for Arnavutköy Town in the coming years [4, 42].

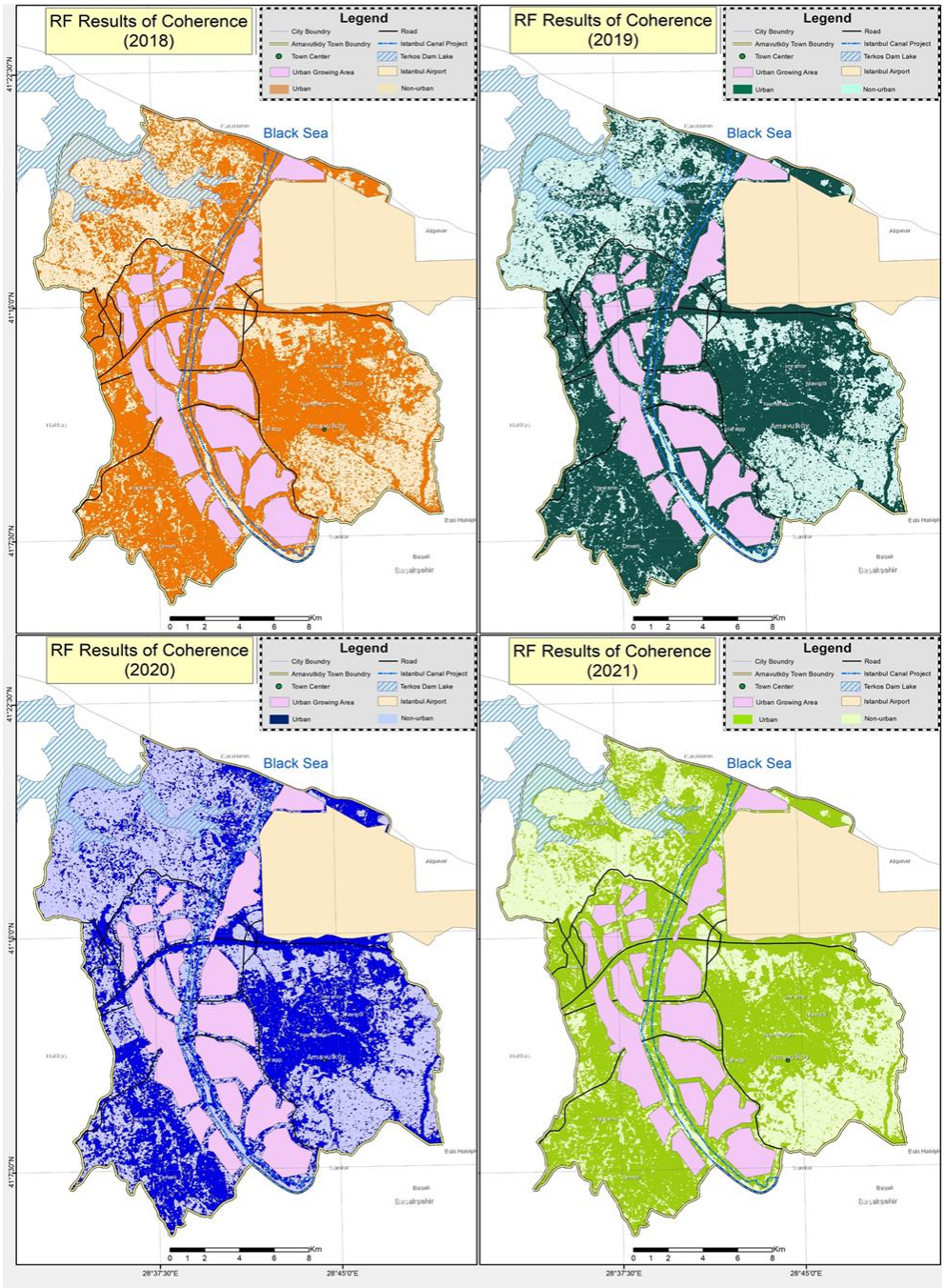

Figure 6. Combine maps of the 1/100.000 scaled environmental plan of the reserve building area of the European side of Istanbul and RF raster maps for each year

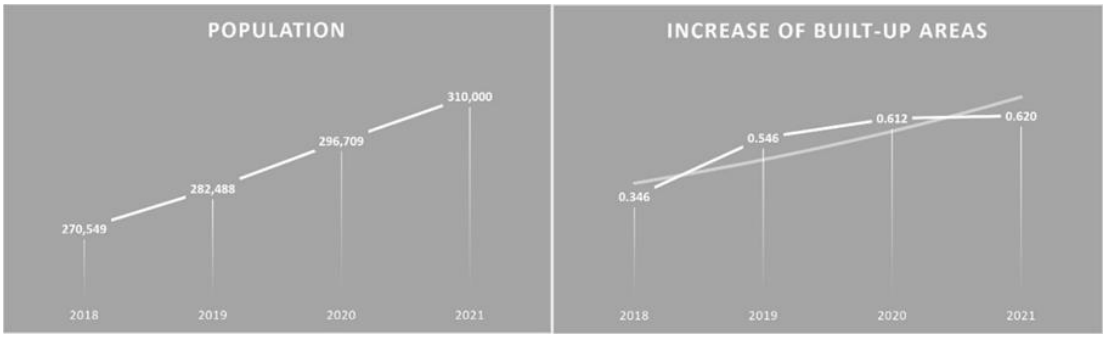

Figure 7. The graphs for changes in population number and BAs rate (%) between 2018 and 2021

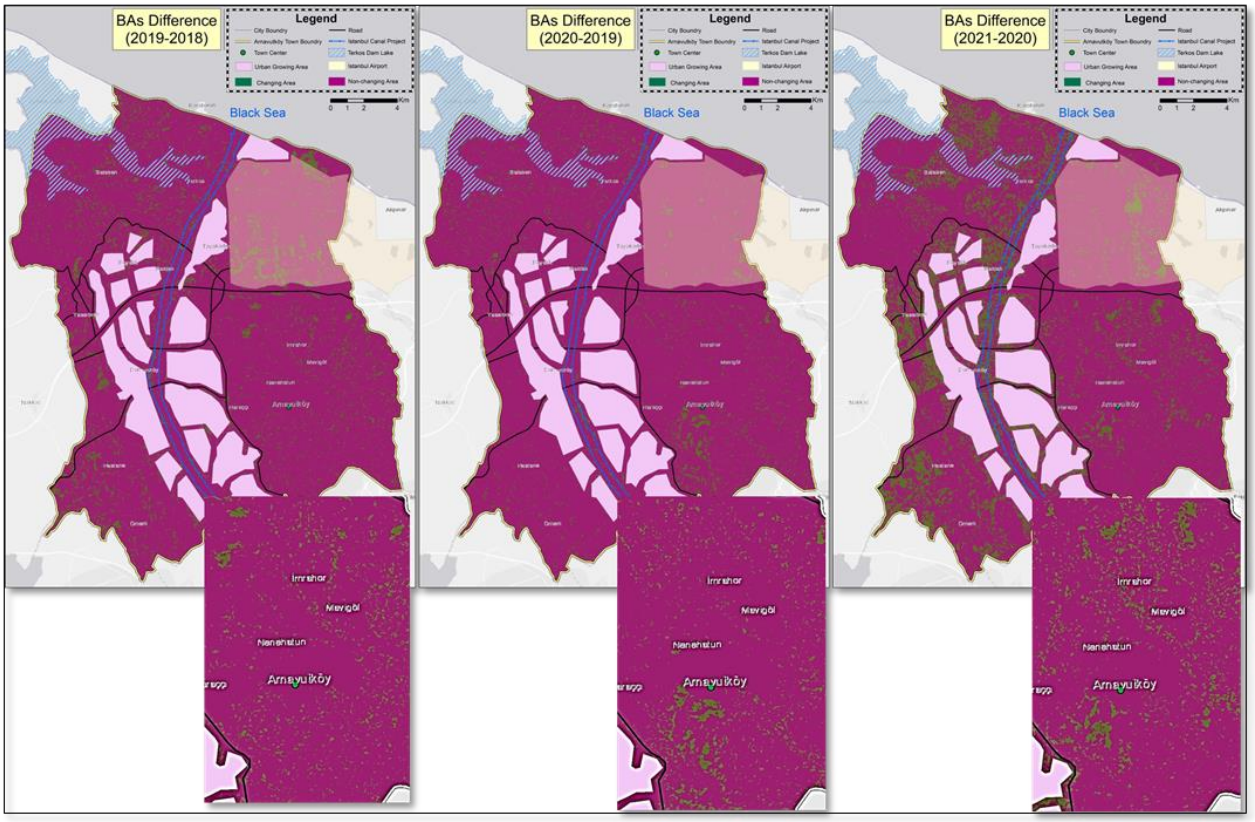

Figure 8. Combine maps of the 1/100.000 scaled environmental plan of the reserve building area of the European side of Istanbul and RF raster maps for each year

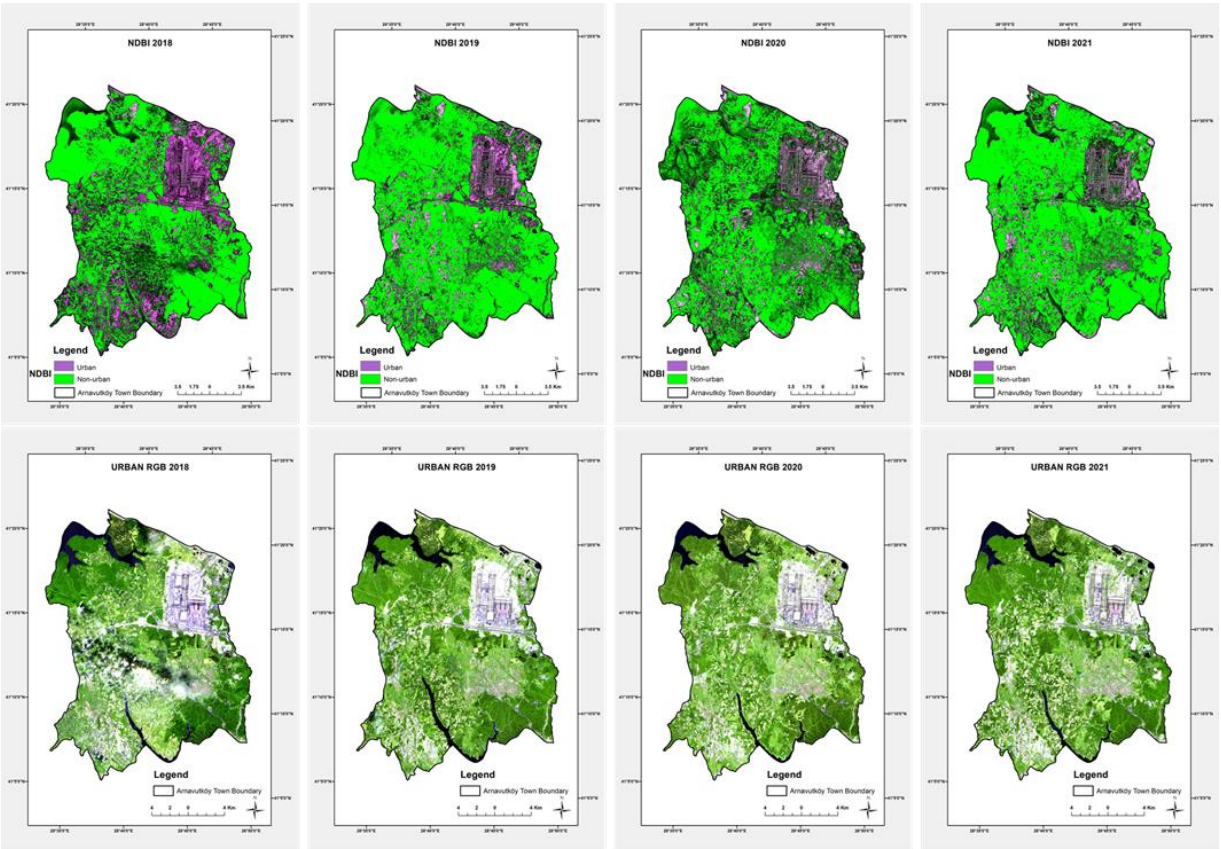

Figure 9. The false color urban RGB composite and the NDBI obtained from Sentinel-2A MSI data

4 Conclusions

After the preprocessing, 15 m of resampled data is obtained from Sentinel-1 radar data. This resolution is often sufficient to distinguish man-made objects. Man-made objects (presented as BAs in this research) express different values as coherence values compared to natural things such as water, tree, and soil. As a result, this difference revealed acceptable results in classification with RF. Based on 2018, the BAs differences in 2019, 2020, and 2021 indicate how rapidly Istanbul's Arnavutköy Town was built in the mentioned years. The highways covering the Great Istanbul Airport and its surroundings were built in the region form the construction mentioned. Most of the Kanal Istanbul megaproject planned for Istanbul covers the boundaries of Arnavutköy Town. Although this project is not yet in the construction phase, Arnavutköy Town has become a center of attraction. The critical point here is how much dense forests and extensive wetlands can be protected.

Acknowledgement

Many thanks to ESA for free SNAP software, Sentinel satellite data, and all kinds of support, and the Republic of Turkey Ministry of Environment and Urbanization for their open-access Spatial Strategy Planning.

Conflict of interest

The author declares that there is no conflict of interest.

Similarity rate (iThenticate): 18%

References

[1] M. Simwanda, Y. Murayama, and M. Ranagalage, Modeling the drivers of urban land use changes in Lusaka, Zambia using multi-criteria evaluation: An analytic network process approach. Land Use Policy, 92: p. 104441, 2020. https://doi.org/10.1016/j.landusepol.2019.104441

[2] X. Li, Y. Zhou, M. Hejazi, M. Wise, C. Vernon, G. Iyer, and W. Chen, Global urban growth between 1870 and 2100 from integrated high resolution mapped data and urban dynamic modeling. Communications Earth & Environment, 2(1), 201, 2021. https://doi.org/10.1038/s43247-021-00273-w

[3] E. Tercan, and U. H. Atasever, Effectiveness of autoencoder for lake area extraction from high-resolution RGB imagery: an experimental study. Environmental Science and Pollution Research, p. 1-13, 2021. https://doi.org/10.1007/s11356-021-12893-y

[4] S. Demir, M. Basaraner, and A.T. Gumus, Selection of suitable parking lot sites in megacities: A case study for four districts of Istanbul. Land Use Policy, p. 105731, 2021. https://doi.org/10.1016/j.landusepol.2021.105731

[5] Y. Lu, L. Yang, K. Yang, Z. Gao, H. Zhou, F. Meng, and J. Qi, A distributionally robust optimization method for passenger flow control strategy and train scheduling on an urban rail transit line. Engineering, 12, 202-220, 2022. https://doi.org/10.1016/j.eng.2021.09.016

[6] Y. Lv, W. Chen, and J. Cheng, Effects of urbanization on energy efficiency in China: New evidence from short run and long run efficiency models. Energy Policy, 147: p. 111858, 2020. https://doi.org/10.1016/j.enpol.2020.111858

[7] A.Varshney, and E. Rajesh, A comparative study of built-up index approaches for automated extraction of built-up regions from remote sensing data. Journal of the Indian Society of Remote Sensing, 42(3): p. 659-663, 2014. https://doi.org/10.1007/s12524-013-0333-9

[8] A. Singh, and S. K. P. Kushwaha, Forest Degradation Assessment Using UAV Optical Photogrammetry and SAR Data. Journal of the Indian Society of Remote Sensing, 49(3): p. 559-567, 2021. https://doi.org/10.1007/s12524-020-01232-2

[9] S. K. Saha, Remote Sensing and Geographic Information System Applications in Hydrocarbon Exploration: A Review. Journal of the Indian Society of Remote Sensing, p. 1-19, 2022. https://doi.org/10.1007/s12524-022-01540-9

[10] H. Cao, H. Zhang, C. Wang, and B. Zhang, Operational built-up areas extraction for cities in China using Sentinel-1 SAR data. Remote Sensing, 10(6), 874, 2018. https://doi.org/10.3390/rs10060874

[11] A. Ghodieh, Urban built-up area estimation and change detection of the occupied West Bank, Palestine, using multi-temporal aerial photographs and satellite images. Journal of the Indian Society of Remote Sensing, 48(2): p. 235-247, 2020. https://doi.org/10.1007/s12524-019-01073-8

[12] R. Guida, A. Iodice, D. Riccio, and U. Stilla, Model-based interpretation of high-resolution SAR images of buildings. IEEE Journal of Selected Topics in Applied Earth Observations and Remote Sensing, 1(2), 107-119, 2008. https://doi.org/10.1109/JSTARS.2008.2001155

[13] M. Massano, E. Macii, A. Lanzini, E. Patti, and L. Bottaccioli, A GIS Open-Data Co-Simulation Platform for Photovoltaic Integration in Residential Urban Areas. Engineering, 2022. https://doi.org/10.1016/j.eng.2022.06.020

[14] A. Htitiou, A. Boudhar, Y. Lebrini, R. Hadria, H. Lionboui, and T. Benabdelouahab, A comparative analysis of different phenological information retrieved from Sentinel-2 time series images to improve crop classification: A machine learning approach. Geocarto International, 37(5), 1426-1449, 2022. https://doi.org/10.1080/10106049.2020.1768593

[15] J. A. Gómez, J. E. Patiño, J. C. Duque, and S. Passos, Spatiotemporal modeling of urban growth using machine learning. Remote Sensing, 12(1), 109, 2019. https://doi.org/10.3390/rs12010109

[16] X. Niu, and Y. Ban, Multi-temporal RADARSAT-2 polarimetric SAR data for urban land-cover classification using an object-based support vector machine and a rule-based approach. International journal of remote sensing, 34(1): p. 1-26, 2013. https://doi.org/10.1080/01431161.2012.700133

[17] L. Bruzzone, M. Marconcini, U. Wegmuller, and A. Wiesmann, An advanced system for the automatic classification of multitemporal SAR images. IEEE Transactions on Geoscience and Remote Sensing, 42(6), 1321-1334, 2004. https://doi.org/10.1109/TGRS.2004.826821

[18] J. Geng, H. Wang, J. Fan, and X. Ma, Deep supervised and contractive neural network for SAR image classification. IEEE Transactions on Geoscience and Remote Sensing, 55(4), 2442-2459, 2017. https://doi.org/10.1109/TGRS.2016.2645226

[19] A. Jamali, and A.A. Rahman, SENTINEL-1 image classification for city extraction based on the support vector machine and random forest algorithms. Int Arch Photogramm Remote Sens Spat Inf Sci, 42(4): p. W16, 2019. https://doi.org/10.5194/isprs-archives-XLII-4-W16-297-2019

[20] B. Wang, J Li, X. Jin, and H. Xiao, Mapping tea plantations from multi-seasonal Landsat-8 OLI imageries using a random forest classifier. Journal of the Indian Society of Remote Sensing, 47, 1315-1329, 2019. https://doi.org/10.1007/s12524-019-01014-5

[21] C. Kar, and S. Banerjee, Tropical Cyclones Intensity Estimation by Feature Fusion and Random Forest Classifier Using Satellite Images. Journal of the Indian Society of Remote Sensing, p. 1-12, 2022. https://doi.org/10.1007/s12524-021-01477-5

[22] H. Wu, J. Zhang, Z. Bao, G. Wang, W. Wang, Y. Yang, and J. Wang, Runoff modeling in ungauged catchments using machine learning algorithm-based model parameters regionalization methodology. Engineering, 2022. https://doi.org/10.1016/j.eng.2021.12.014

[23] P.O. Gislason, J.A. Benediktsson, and J.R. Sveinsson, Random forests for land cover classification. Pattern recognition letters, 27(4): p. 294-300, 2006. https://doi.org/10.1016/j.patrec.2005.08.011

[24] J. Sharma, J. Eppler, and J. Busler, Urban infrastructure monitoring with a spatially adaptive multi-looking InSAR technique. Proc. of Fringe, Frascati, Italy, 2015.

[25] H. B. Makineci, and H. Karabörk, Evaluation digital elevation model generated by synthetic aperture radar data. International Archives of the Photogrammetry, Remote Sensing and Spatial Information Sciences, 1: p. 57-62, 2016. https://doi.org/10.5194/isprs-archives-XLI-B1-57-2016

[26] Y. Ban, A. Jacob, and P. Gamba, Spaceborne SAR data for global urban mapping at 30 m resolution using a robust urban extractor. ISPRS Journal of Photogrammetry and Remote Sensing, 103: p. 28-37, 2015. https://doi.org/10.1016/j.isprsjprs.2014.08.004

[27] Y. Yao, D. Chen, L. Chen, H. Wang, and Q. Guan, A time series of urban extent in China using DSMP/OLS nighttime light data. PLoS One, 13(5), e0198189, 2018. https://doi.org/10.1371/journal.pone.0198189

[28] F. Li, Q. Yan, Z. Bian, B. Liu, and Z. Wu, A POI and LST adjusted NTL urban index for urban built-up area extraction. Sensors, 20(10), 2918, 2020. https://doi.org/10.3390/s20102918

[29] Z. Jun, Y. Xiao-Die, and L. Han, The extraction of urban built-up areas by integrating night-time light and POI data—A case study of Kunming, China. IEEE Access, 9: p. 22417-22429, 2021. https://doi.org/10.1109/ACCESS.2021.3054169

[30] A. Braun, Retrieval of digital elevation models from Sentinel-1 radar data–open applications, techniques, and limitations. Open Geosciences, 13(1): p. 532-569, 2021. https://doi.org/10.1515/geo-2020-0246

[31] A. Mercier, J. Betbeder, F. Rumiano, J. Baudry, V. Gond, L. Blanc, C. Bourgoin, G. Cornu, C. Ciudad, M. Marchamalo, R. Poccard-Chapuis, and L. Hubert-Moy, Evaluation of Sentinel-1 and 2 Time Series for Land Cover Classification of Forest–Agriculture Mosaics in Temperate and Tropical Landscapes. Remote Sensing, 11, 979, 2019. https://doi.org/10.3390/rs11080979

[32] L. Carrasco, A. W. O'Neil, R.D. Morton, and C. S. Rowland, Evaluating combinations of temporally aggregated Sentinel-1, Sentinel-2 and Landsat 8 for land cover mapping with Google Earth Engine. Remote Sensing, 11(3), 288, 2019. https://doi.org/10.3390/rs11030288

[33] A. Semenzato, S. E. Pappalardo, D. Codato, U. Trivelloni, S. De Zorzi, S. Ferrari, M. De Marchi, and M. Massironi, Mapping and Monitoring Urban Environment through Sentinel-1 SAR Data: A Case Study in the Veneto Region (Italy). ISPRS Int. J. Geo-Inf., 9, 375, 2020. https://doi.org/10.3390/ijgi9060375

[34] D. Colson, G.P. Petropoulos, and K.P. Ferentinos, Exploring the potential of Sentinels-1 & 2 of the Copernicus Mission in support of rapid and cost-effective wildfire assessment. International journal of applied earth observation and geoinformation, 73: p. 262-276, 2018. https://doi.org/10.1016/j.jag.2018.06.011

[35] H. Karabörk, H. B. Makineci, O. Orhan, and P. Karakus, Accuracy assessment of DEMs derived from multiple SAR data using the InSAR technique. Arabian Journal for Science and Engineering, 46, 5755-5765, 2021. https://doi.org/10.1007/s13369-020-05128-8

[36] S. Niculescu, J. Xia, D. Roberts, and A. Billey, Rotation Forests and Random Forest classifiers for monitoring of vegetation in Pays de Brest (France). The International Archives of Photogrammetry, Remote Sensing and Spatial Information Sciences, 43, 727-732, 2020. https://doi.org/10.5194/isprs-archives-XLIII-B3-2020-727-2020

[37] T. T. H. Nguyen, T. N. Q. Chau, T. A. Pham, T. X. P. Tran, T. H. Phan, and T. M. T. Pham, Mapping Land use/land cover using a combination of Radar Sentinel-1A and Sentinel-2A optical images. In IOP Conference Series: Earth and Environmental Science (Vol. 652, No. 1, p. 012021). IOP Publishing, 2021. https://doi:10.1088/1755-1315/652/1/012021

[38] A. R. As-Syakur, I. W. S. Adnyana, I. W. Arthana, and I. W. Nuarsa, Enhanced built-up and bareness index (EBBI) for mapping built-up and bare land in an urban area. Remote sensing, 4(10), 2957-2970, 2012. https://doi.org/10.3390/rs4102957

[39] P. Ettehadi Osgouei, S. Kaya, E. Sertel, and U. Alganci, Separating built-up areas from bare land in mediterranean cities using Sentinel-2A imagery. Remote Sensing, 11(3), 345, 2019. https://doi.org/10.3390/rs11030345

[40] C. Yang, Remote Sensing and Precision Agriculture Technologies for Crop Disease Detection and Management with a Practical Application Example. Engineering, 6(5): p. 528-532, 2020. https://doi.org/10.1016/j.eng.2019.10.015

[41] K. Getu, and H.G. Bhat, Analysis of spatio-temporal dynamics of urban sprawl and growth pattern using geospatial technologies and landscape metrics in Bahir Dar, Northwest Ethiopia. Land Use Policy, 109: p. 105676, 2021. https://doi.org/10.1016/j.landusepol.2021.105676

[42] E. Ustaoglu, and A.C. Aydınoglu, Suitability evaluation of urban construction land in Pendik district of Istanbul, Turkey. Land Use Policy, 99: p. 104783, 2020. https://doi.org/10.1016/j.landusepol.2020.104783

[43] M.C. Peel, B.L. Finlayson, and T.A. McMahon, Updated world map of the Köppen-Geiger climate classification. Hydrol. Earth Syst. Sci., 11(5): p. 1633-1644, 2007. https://doi.org/10.5194/hess-11-1633-2007

[44] T. Kindap, A severe sea-effect snow episode over the city of Istanbul. Natural Hazards, 54(3): p. 707-723, 2010. https://doi.org/10.1007/s11069-009-9496-7

[45] S.A. Swalih, and E. Kahya, Performance of gridded precipitation products in the Black Sea region for hydrological studies. Theoretical and Applied Climatology, 149(1): p. 465-485, 2022. https://doi.org/10.1007/s00704-022-04054-z

[46] D. Amitrano, G. Di Martino, R. Guida P. Iervolino, A. Iodice, M. N. Papa, D. Riccio, and G. Ruello, Earth Environmental Monitoring Using Multi-Temporal Synthetic Aperture Radar: A Critical Review of Selected Applications. Remote Sens., 13, 604, 2021. https://doi.org/10.3390/rs13040604

[47] D. Amitrano, F. Cecinati, G. Di Martino, A. Iodice, D. Riccio, and G. Ruello, Urban areas extraction from multitemporal SAR RGB images using interferometric coherence and textural information. In Fringe 2015 Workshop, 2015. European Space Agency.

[48] M. Stasolla, and P. Gamba, Spatial indexes for the extraction of formal and informal human settlements from high-resolution SAR images. IEEE Journal of Selected Topics in Applied Earth Observations and Remote Sensing, 1(2): p. 98-106, 2008. https://doi.org/10.1109/JSTARS.2008.921099

[49] W. K. Baek, and H. S. Jung, Precise Three-Dimensional Deformation Retrieval in Large and Complex Deformation Areas via Integration of Offset-Based Unwrapping and Improved Multiple-Aperture SAR Interferometry: Application to the 2016 Kumamoto Earthquake. Engineering, 6(8): p. 927-935, 2020. https://doi.org/10.1016/j.eng.2020.06.012

[50] A.W. Jacob, F. Vicente-Guijalba, C. Lopez-Martinez, J.M. Lopez-Sanchez, M. Litzinger, H. Kristen, A. Mestre-Quereda, D. Ziółkowski, M. Lavalle, C. Notarnicola, G. Suresh, O. Antropov, S. Ge, J. Praks, Y. Ban, E. Pottier, J.J. Mallorqu Franquet, J. Duro, M.E. Engdahl, Sentinel-1 InSAR coherence for land cover mapping: a comparison of multiple feature-based classifiers, IEEE J. Select. Topics Appl. Earth Observ. Remote Sens., 13, pp. 535-552, 2020. https://doi.org/10.1109/JSTARS.2019.2958847

[51] L. Breiman, Random Forests--Random Features. UC Berkeley TR567, 1999. Statistics Department, Berkeley, USA, Technical Report 567, September 1999.

[52] L. Breiman, Random forests. Machine learning, 45(1): p. 5-32, 2001. https://doi.org/10.1023/A:1010933404324

[53] S. Abdikan, C. Bayik, F. Balık Sanli, and M. Ustuner, An Assessment of Urban Area Extraction Using ALOS-2 Data. In 2019 9th International Conference on Recent Advances in Space Technologies (RAST) (pp. 403-406). IEEE, 2019. https://doi.org/10.1109/RAST.2019.8767819

[54] F. Calò, S. Abdikan, T. Görüm, A. Pepe, H. Kiliç, and F. Balik Şanli, The space-borne SBAS-DInSAR technique as a supporting tool for sustainable urban policies: The case of Istanbul Megacity, Turkey. Remote Sensing, 7(12), 16519-16536, 2015. https://doi.org/10.3390/rs71215842